NASA TECHNICAL MEMORANDUM

NASA TM X-64692

EXPERIMENT POINTING CONTROL DURING SPACE SHUTTLE SORTIE MISSIONS

By P. D. Nicaise
Preliminary Design Office
Program Development

January 31, 1972

NASA

George C. Marshall Space Flight Center
Marshall Space Flight Center, Alabama

TECHNICAL REPORT STANDARD TITLE PAGE

1. REPORT NO. TM X - 64692	2. GOVERNMENT ACCESSION NO.	3. RECIPIENT'S CATALOG NO.
4. TITLE AND SUBTITLE Experiment Pointing Control During Space Shuttle Sortie Missions		5. REPORT DATE January 31, 1972
		6. PERFORMING ORGANIZATION CODE PD-DO-ES
7. AUTHOR(S) P. D. Nicaise		8. PERFORMING ORGANIZATION REPORT #
9. PERFORMING ORGANIZATION NAME AND ADDRESS George C. Marshall Space Flight Center Marshall Space Flight Center, Alabama 35812		10. WORK UNIT NO.
		11. CONTRACT OR GRANT NO.
		13. TYPE OF REPORT & PERIOD COVERED Technical Memorandum
12. SPONSORING AGENCY NAME AND ADDRESS National Aeronautics and Space Administration Washington, D.C. 20546		14. SPONSORING AGENCY CODE

15. SUPPLEMENTARY NOTES

Prepared by the Navigation and Control Systems Branch, Electronics and Controls Division, Preliminary Design Office, Program Development

16. ABSTRACT

The pointing and stability problems of the Sortie mission are examined from the standpoint of basic Shuttle capability and the techniques that could be used for improving this capability to accommodate a maximum number of experiments. Augmentation of the basic Shuttle control system is proposed to provide an acceptable pointing environment. A stabilized reference base is recommended as a general pointing instrument for certain earth observation and astronomy experiments. Simulation results are presented which were obtained by modeling the Skylab Experiment Pointing Control (EPC) system on a thruster controlled Shuttle.

17. KEY WORDS Space Shuttle Payloads Orbital Stabilization Experiment Pointing Control Thruster Propellant Consumption Momentum Management	18. DISTRIBUTION STATEMENT STAR Announcement ERICH E. GOERNER Director, Preliminary Design Office

19. SECURITY CLASSIF. (of this report)	20. SECURITY CLASSIF. (of this page)	21. NO. OF PAGES	22. PRICE
Unclassified	Unclassified	34	$ 3.00

MSFC - Form 3292 (May 1969)

ACKNOWLEDGMENT

The author gratefully acknowledges the contribution of Manuel Key in the analog computer programming, operation and data analysis associated with the simulation task. In addition, personal communications with Paul Golley, Charles Cornelius, Henning Krome, Fred Applegate, and Paul Fisher of Astrionics Laboratory, Science and Engineering, and Robert Shelton and Rufus Passwater of Sperry Rand Corporation furnished invaluable information on Skylab operation and performance.

TABLE OF CONTENTS

LIST OF ILLUSTRATIONS

LIST OF TABLES

DEFINITION OF SYMBOLS

A_0	Position control gain
A_1	Rate control gain
d	Offset between the EPC gimbal axis and C.G.
$F\Delta t$	Thruster minimum impulse
H_{gg}	Angular momentum from gravity gradient torques
H_s	Position control gain of EPC
I_{sp}	Specific impulse
K	Spring constant between EPC and Shuttle
K_A	Amplifier gain
K_M	Motor gain
K_1	Rate control gain of EPC
K_0	Position gain of experiment table
ℓ	Lever arm between Shuttle C.G. and EPC gimbal axis
L	Lever arm between Shuttle C.G. and thruster location
M_E	Mass of EPC
$\dot{M}_{gg}$	Propellant consumption rate resulting from gravity gradient torques
$\dot{M}_{LC}$	Propellant consumption rate resulting from undisturbed limit cycle
S	LaPlace operator
T_c	Control torque
T_f	Friction torque

DEFINITION OF SYMBOLS (Concluded)

$\left.\begin{matrix}\alpha \\ \beta \\ \gamma\end{matrix}\right\}$	Angular deviation about vehicle axes (X, Y, Z) relative to the reference orbital orientation
δ	Angular deviation of the EPC system relative to inertial space
θ	Angle between Shuttle and EPC system
$\sum \Delta\phi_s$	Sum of the velocity changes about all three axes resulting from minimum thruster firing
τ_a	EPC servo loop time constant
ϕ_s	Angular deviation of the Shuttle relative to inertial space
ϕ_{DB}	Shuttle thruster deadband
Φ_s	Moment of inertia of the Shuttle
Φ_E	Moment of inertia of the EPC package

DEFINITION OF ACRONYMNS

ACPS	Attitude Control Propulsion system
C.G.	Center of gravity
CMGs	Control Moment Gyros
EPC	Experiment Pointing Control (as on Skylab)
IOP	In the orbital plane
LV	Local vertical
POP	Perpendicular to the orbital plane

EXPERIMENT POINTING CONTROL DURING SPACE SHUTTLE SORTIE MISSIONS

INTRODUCTION

The Space Shuttle is being planned with the capability for remaining on orbit during an interval of several days while operating as a research station and experiment base. This mode of operation is known as a Sortie mission. Some advantages of the Sortie mission are direct participation of the research scientist in the experiments, mission to mission replacement or modification of equipment, and rapid recovery of all data and equipment. These advantages should establish the Sortie mission as a standard method for performing many orbital experiments. Other methods, such as free flying modules, must be used to accommodate experiments which require higher orbits, longer on orbit times, lower environmental contamination or higher stability levels than can be achieved on a Sortie mission.

This report is concerned with the pointing accuracy and stability potential of Shuttle based instruments during the Sortie mission. Figure 1 illustrates the error types and defines the relationship between line of sight errors. Pointing accuracy refers to the ability to achieve and maintain an orientation relative to a particular observation point. Pointing errors are a combination of reference errors which result from sensor inaccuracy or unknown misalignments between sensors and experiment, and stability errors which generally result from deadband or other characteristic servo loop errors. Stability error is defined as the angular deviation during a given operational interval. Jitter rate is the maximum instantaneous angular velocity expected during a pointing experiment. These pointing characteristics should define the capability of the Shuttle to a level which would be useful to the researcher when considering the Shuttle as a candidate vehicle for a particular experiment.

BASIC SHUTTLE STABILITY CHARACTERISTICS

The Attitude Control Propulsion System (ACPS) presently proposed for the Shuttle consists of about thirty 1000 lb thrusters for translational trim

● ROLL ABOUT LINE OF SIGHT IS A POINTING ERROR WHICH IS NOT REPRESENTED ON THIS DIAGRAM. THE NATURE OF THIS ERROR DEPENDS ON THE PARTICULAR CONFIGURATION OF THE POINTING SYSTEM.

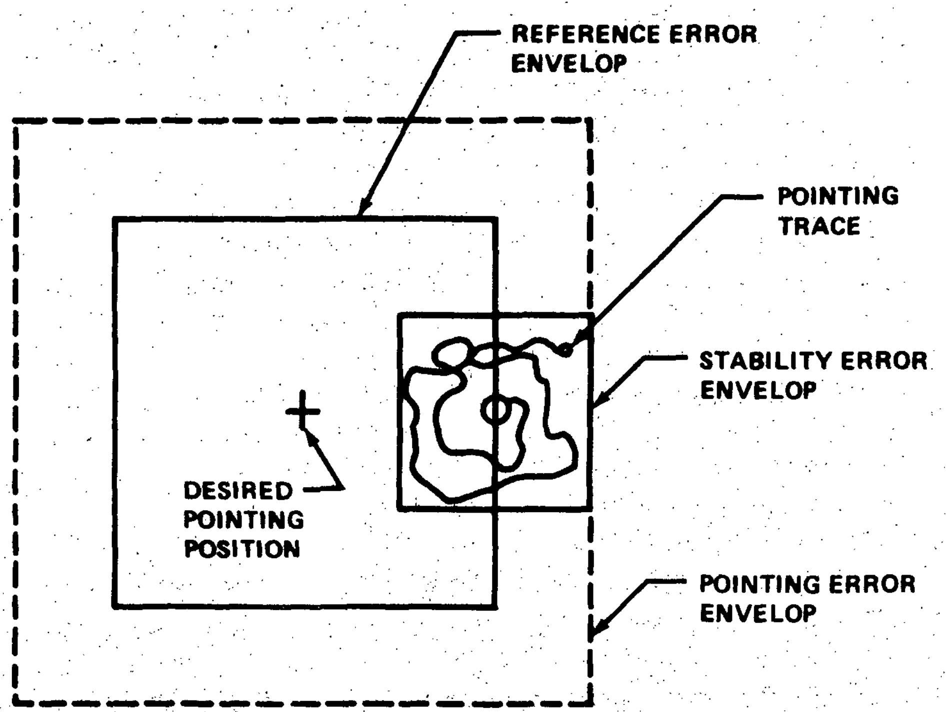

Figure 1. Pointing and stability error definitions.

maneuvers and rotational control. The minimum angular acceleration (single thruster firing) provided by the ACPS is typically about 1 degree/s^2. This value is established by the control torque requirement during reentry and does not furnish efficient operation or a high level of stability for orbital control. Although this condition is probably acceptable when the Shuttle operates as a payload transport, it is not satisfactory when the Shuttle is serving as an experiment base. Propellant consumption from limit cycling is very high, the large volume of ACPS reaction products interferes with optical experiments, thruster translational acceleration exceeds the requirement for life science experiments, the angular acceleration makes precision pointing with servo driven tables difficult or impossible, and the residual angular velocity (about 0.1 degree/s) exceeds some experiment requirements and makes any transition to CMG control very expensive in terms of momentum (about 10 000 ft-lb-s). Figure 2 shows the maximum propellant rate for single thruster limit cycle operation and compares large (1000 lb) thrusters with small

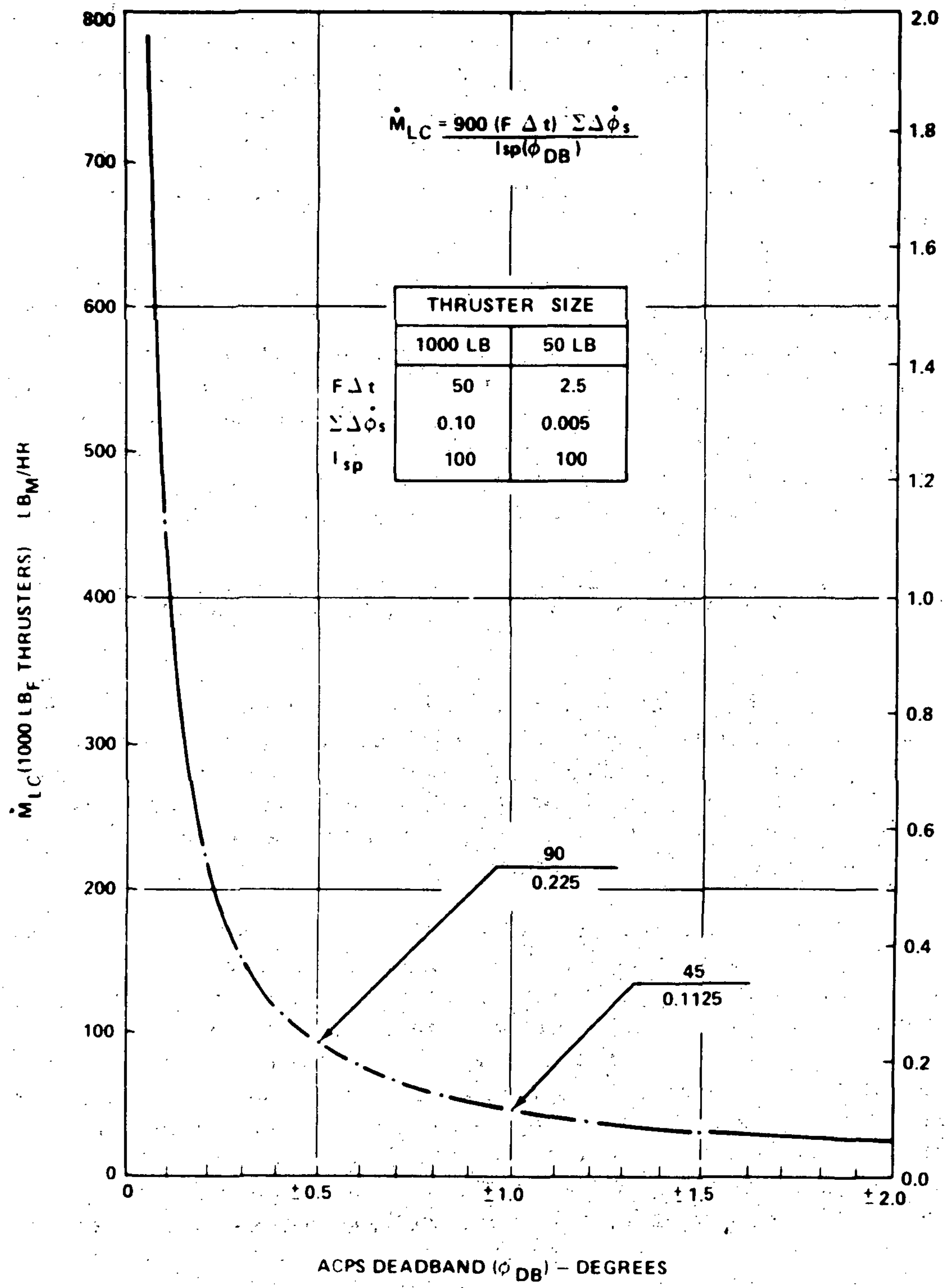

Figure 2. Maximum propellant consumption rate for undisturbed limit cycle.

(50 lb) thrusters that are properly sized for orbital control. This curve also shows the relationship between propellant consumption and ACPS deadband. Since deadband is the primary contributor to stability errors, the curve is a direct indicator of propellant consumption rate necessary to maintain a particular stability level. Figure 2 is based on an I_{sp} value of 100 s to normalize the curve and make it easy to calculate propellant rate for any particular I_{sp} value.

There are some changes which could be made to the thruster logic to reduce residual angular rates and propellant consumption of large thrusters. One method is to use "differential thrusting" in which two thrusters act in opposition for slightly different on times to produce a small resulting impulse. Another method is to define a control law which produces an unsymmetrical limit cycle with alternate firings producing very low rates. However, these techniques will not reduce the angular or translational acceleration levels and the additional complications make them of questionable value.

IMPROVEMENT OF SHUTTLE ORBITAL CONTROL CHARACTERISTICS

The deficiencies of the Shuttle ACPS for the Sortie mission can be most effectively overcome by using a separate control system which has been specifically sized for the task of orbital stabilization. The two prime contenders are small (about 50 lb) thrusters or control moment gyros (CMGs). To properly evaluate these two methods, some consideration must be given to the control moment requirements for a Sortie mission.

Figure 3 illustrates the basic vehicle orientations to the orbital plane which could be used to meet various experiment objectives. The inertial reference orientations are best suited to astronomy experiments. The case for which the vehicle X-axis is perpendicular to the orbit plane (X-POP) provides a relatively low angular momentum accumulation from gravity gradient torques as shown by the expressions in the first column. However, this mode restricts the vehicle attitude and requires onboard equipment to provide pointing out of the plane of the orbit. The vehicle X-axis in the orbit plane (X-IOP) allows all sky pointing by the vehicle, but the angular momentum accumulation is very high. Other orientations, such as X-axis 45 degrees to orbit plane, produce even higher accumulation but without any gain in pointing capability. The cyclic momentum components have a periodic nature with maximum values every quarter orbit. The secular momentum components accumulate continuously and the CMGs must be desaturated at regular intervals by an opposing torque (momentum "dumping").

ORBITAL ALTITUDE	VEHICLE ORIENTATION		INERTIAL REFERENCE		EARTH REFERENCE	
			X-POP	X-IOP	X-LV	Y,Z-LV
			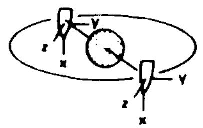	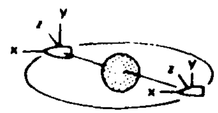	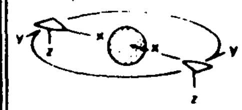	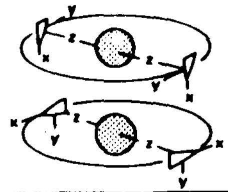
100 N. MILES	CYCLIC MOMENTUM PER 1/4 ORBIT	X	569	0	0	0
		Y	0	15942 cos α	0	0
		Z	0	16512 sin α	0	0
	SECULAR MOMENTUM PER ORBIT	X	0	1789 sin 2 α	0	3578 sin 2 α
		Y	1748 β	1748 β sin α	3496 β	3496 β cos α
		Z	1811 γ	1811 γ cos α	3622 γ	3622 γ sin α
	TOTAL (RSS)		2580	16604	5034	3622
270 N. MILES	CYCLIC MOMENTUM PER 1/4 ORBIT	X	530	0	0	0
		Y	0	14860 cos α	0	0
		Z	0	15390 sin α	0	0
	SECULAR MOMENTUM PER ORBIT	X	0	1670 sin 2 α	0	3340 sin 2 α
		Y	1630 β	1630 β sin α	3260 β	3260 β cos α
		Z	1688 γ	1688 γ cos α	3376 γ	3376 γ sin α
	TOTAL (RSS)		2406	15477	4693	3376

- ANGULAR MOMENTUM IS EXPRESSED IN FT-LB-S, ANGLES ARE IN DEGREES.
- α, β AND γ ARE ROTATIONS ABOUT X, Y AND Z AXES RESPECTIVELY.
- β AND γ ARE RESTRICTED TO SMALL ANGLES.
- UNITY ANGLES ($\alpha, \beta, \gamma = 1^{\circ}$) WERE ASSUMED IN CALCULATING TOTAL MOMENTUM

Figure 3. Angular momentum accumulation for standard orientations relative to the orbital plane.

The earth reference orientations are best suited for earth observation missions. The case for which the vehicle Z-axis is along the local vertical (Z-LV) appears to have the advantage for maximum viewing and minimum angular momentum accumulation. However, thermal or other constraints may dictate the Y-LV or X-LV orientation. Note that the Y-LV and the Z-LV cases result in essentially the same accumulation. There are no cyclic momentum values for earth referenced orientations.

The total momentum values are calculated by assuming angular dispersions of 1 degree about the reference orientations and taking the root sum square (RSS) of the components. This provides a reasonable error value and makes it convenient for establishing CMG requirements.

Aerodynamic forces are generally neglected for the 270 nautical mile orbit but can create significant disturbing moments in the 100 nautical mile orbit. However, the magnitude of these moments are highly dependent on vehicle configuration and orientation. Therefore, aerodynamic torques will be neglected in the following comparison.

Now that the most likely vehicle orientations have been defined and control moment requirements established, it is possible to compare CMG capability with the small thrusters. The first basis of comparison will be weight. Figure 4 shows CMG weights as a function of control moment requirements. These are approximate weights for the wheel, gimbals and associated hardware but do not include electronic boxes, cables, or peripheral equipment. The excluded items should be a relatively insignificant portion of the total weight. One trace gives the number, weight, and volume for Skylab CMGs. The other trace is for a larger CMG presently under development by the Bendix Corporation for the Astrionics Laboratory.

Table 1 is a table of propellant consumption rates that would result from gravity gradient torques. These values are constructed from the effective angular momentum (H_{gg}) per axis as defined in Figure 3. A vehicle misalignment of 1 degree to the reference orientation was assumed. The distance from thrusters to center of mass was taken as 45 ft for roll (ℓ_x) and as 55 ft for pitch and yaw (ℓ_y and ℓ_z).

Table 2 is a comparison of CMGs with small thrusters on the basis of weight. The data show the estimated weights for a typical mission (270 nautical mile orbit) at all the standard orientations. The propellant consumption rates are given for the thrusters on the first three lines. The propellant weight is calculated from these rates for a 7 day mission which is continuously

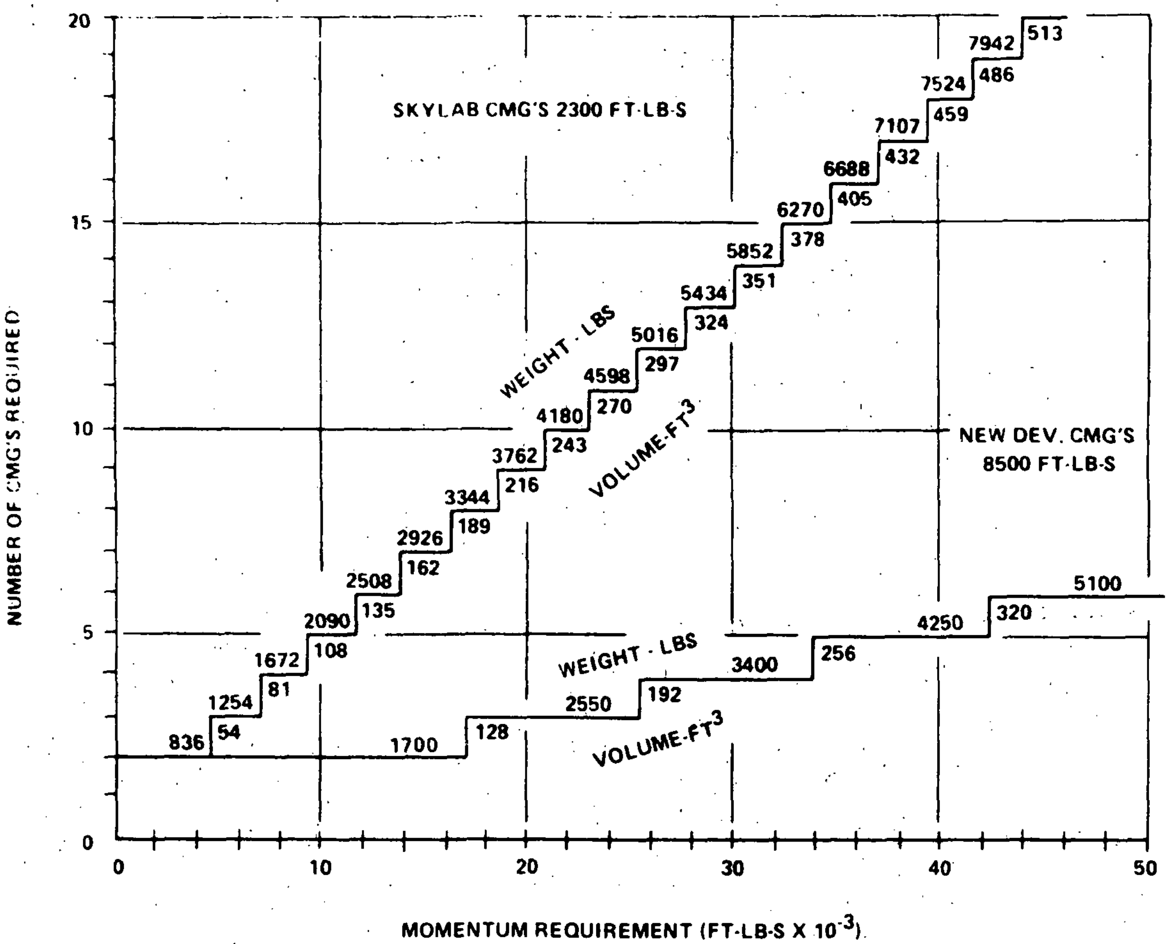

Figure 4. CMG requirements.

pointed with a deadband (Φ_{DB}) of ±0.5 degree. Total thruster system weight includes propellant weight plus 300 lb of estimated thruster hardware weight. The results indicate that both sizes of CMGs are significantly heavier than the thruster system for all orientations.

The second criteria for comparison will be stability and jitter rate. Skylab performance (including sensor noise) is expected to be about ±7.5 arc min (±0.125 degree) and ±1 arc min/s (±0.0167 degree/s) for the CMG controlled cluster. The small thrusters will provide rates below 0.01 degree/s and can be operated with a deadband of ±0.125 degree (with ideal sensor inputs) at a propellant consumption rate of 0.9 lb/hr (I_{sp} = 100 s).

This rate results in about 150 lb of propellant when the vehicle is restrained

TABLE 1. PROPELLANT CONSUMPTION RATES FROM GRAVITY GRADIENT TORQUES

- VALUES IN THE TABLE ARE LBS/HR.

ORBITAL ALTITUDE (NAUTICAL MILES)	VEHICLE ORIENTATION TO ORBITAL PLANE			
	X-POP	X-IOP	X-LV	Y,Z-LV
100	0.77	8.37	0.86	0.46
270	0.72	7.78	0.83	0.43

$$\dot{M}_{gg} = \frac{\dot{H}_{gg}}{1.5\ L\ I_{sp}} \left(\frac{LB.}{HR}\right)$$

$L_x = 45$ ft

$L_{y,z} = 55$ ft

$I_{sp} = 100s$

$\varphi, \beta, \gamma = 1^o$

TABLE 2. WEIGHT COMPARISON CMGs VERSUS SMALL THRUSTERS

WEIGHT CONTRIBUTORS	VEHICLE ORIENTATIONS IN ORBIT			
	X-POP	X-IOP	X-LV	Y,Z-LV
PROPELLANT CONSUMPTION RATES (LB/HR)				
$\dot{M}_{LC}$ (UNDISTURBED LIMIT CYCLE) $\phi_{DB} = \pm 0.5^o$	0.11	0.11	0.11	0.11
$\dot{M}_{gg}$ (GRAVITY GRADIENT TORQUES) 270 N. MILE	0.36	3.89	0.42	0.22
TOTAL $\dot{M}$ (50LB THRUSTERS, $I_{sp} = 200S$)	0.47	4.00	0.53	0.33
PROPELLANT WEIGHT (LBS) FOR A 7 DAY MISSION	79	672	89	55
ESTIMATED THRUSTER HARDWARE WEIGHT ≤	300	300	300	300
TOTAL THRUSTER SYSTEM WEIGHT (LBS)	379	972	389	355
SKYLAB CMG WEIGHT (LBS)	836	3344	1254	1254
NEW DEVELOPMENT CMG WEIGHT (LBS)	1700	2550	1700	1700

in the ± 0.125 degree deadband for the entire seven day mission. Thruster system weight is still significantly less than CMG weight for pointing accuracy equivalent to the Skylab cluster. Although the absolute accuracy of CMGs probably does exceed that of the small thrusters, this is a relatively insignificant advantage since reference errors and sensor noise become the predominant error sources for such high accuracy pointing of the airframe.

The third criteria for comparison will be contamination of the space environment. On this point, the CMGs obviously have the advantage since they will not produce any contaminants provided their accumulated momentum can be desaturated by gravity gradient torques. However, this also implies that a portion of each orbit may have to be devoted to maneuvering to a particular orientation in the gravitational field. The CMGs may also be dumped by using thrusters but the amount of contamination must then be charged to the CMGs. When the actual contamination level of small thrusters is given objective consideration, it becomes obvious that their contribution to the total problem is not large and may be insignificant. This is especially true if thruster orientation is directed away from the experiment line of sight and thrusters use "clean" reactants which do not impinge on the vehicle structure. Thruster reactants tend to leave the vicinity of the vehicle at high velocity and do not contribute to the "space cloud" in the same manner as leakage and outgassing. The actual mass expelled by the thrusters is only about 1 lb/hr (1.5 lb/orbit) or less than 200 lb for a 7 day mission.

The final criteria for comparison will be cost and complexity. The thrusters appear to have the advantage because they are simpler from both the electrical and mechanical standpoint. In addition, a CMG system actually needs a low thrust system to null vehicle rates prior to turning control over to the CMGs. Otherwise, the CMGs must be oversized to compensate for residual rates (± 0.1 degree/s) left on the vehicle by minimum firing of the Shuttle (1000 lb thrusters) ACPS. The necessary increase in CMG capability (about 10 000 ft-lb-s) would depend on which orientation they were originally sized for but it could be as much as a 400 percent increase. Therefore, it appears that if an efficiently sized CMG system is to be employed, it should be used in conjunction with a small thruster system.

The small thrusters have an undeniable advantage over large thrusters or CMGs as a means of stabilizing the Shuttle for presently defined sortie missions. CMGs would have a distinct advantage only for very long missions (several weeks or months) with orientations that have significant cyclic momentum components.

A STABILIZED REFERENCE BASE FOR PRECISION POINTING OF EXPERIMENTS

The improvement of Shuttle orbital stability characteristics, as discussed in the preceding text, is necessary for most of the proposed sortie experiments. However, many experiments will require tracking capability, multiple pointing directions, pointing accuracy, stability levels and jitter rates far beyond the capability of even the improved Shuttle control system. Precision experiment pointing cannot be accomplished by attaching experiments directly to the Shuttle airframe or by bases which simply rotate by open loop command (crank around bases). Many experiments may have internal optical stabilization or individual tables to meet their particular requirements. This is an especially satisfactory arrangement when the experiments need to be in or near the pressurized experiment laboratory. However, it appears that a general experiment platform could be provided which would have a level of convenience and flexibility that would be impractical for individual platforms. Such a platform could be planned with the capability for precision pointing (about 1 arc sec) of several small experiments or a single very large experiment. It could eliminate the requirement for at least some of the specialized experiment tables which would result if each experimenter had to provide his own pointing system. In addition, a standard table would provide an easier interface for such support items as the computer and TV display.

Figure 5 is an illustration of an experiment table which should meet the objectives discussed in the previous paragraph. It has a conventional gimbaled torquer controlled inner ring that provides control about two axes. This stabilizes the line-of-sight with roll about the line-of-sight depending on the Shuttle airframe stability. This pointing concept is the same as that for Skylab except this gimbal system must point through a larger range of angles and the Skylab inner gimbal is used for roll about line-of-sight. The outer and middle gimbal order is somewhat arbitary, but is arranged as shown to accommodate very large experiments whose lengths could exceed the diameter of the payload bay. The experiment could be placed in the inner gimbal ring with its long axis aligned with the long axis of the bay. The gimbal torquers could then rotate the experiment out of the bay for observations.

The conventional gimbal system recommended for this table does not have the ideal pointing characteristics of a gas bearing or even a flex pivot. One of the problems is the stiction and friction characteristics associated with the gimbal bearings. However, the practical advantages of a relatively

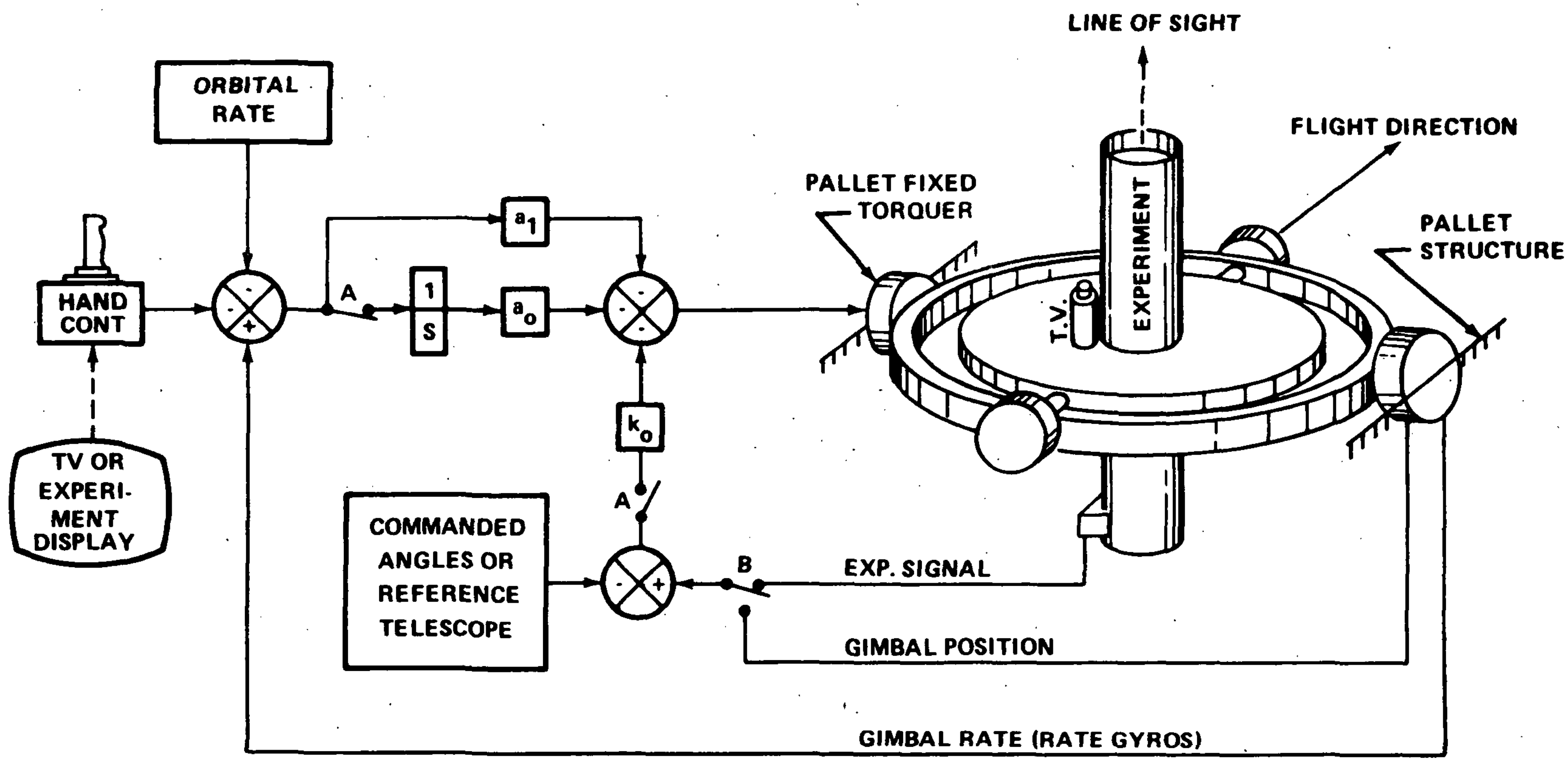

Figure 5. Experiment table pointing control.

simple design which can rotate through large angles without the need for a gas bearing operating in the space environment is an attractive option. The only question is whether it can meet the precision pointing requirements of 1 arc sec or less. The best existing design for comparison is probably the large table in the Astrionics Simulation Laboratory. This table achieves repeatable pointing accuracy of about 1 arc sec. A table which has been specifically designed to operate in a lower gravitational environment could be expected to provide considerably better accuracy. Therefore, for the general experiment pointing task, a conventional gimbaled table should meet the requirements at minimum risk and expense.

The signal flow is shown in Figure 5 to illustrate some of the flexibility and convenience that the table can furnish to the experimenter. The gimbal rate loop, with switch A as shown, provides the torquer commands to inertially stabilize the experiment base and isolate it from Shuttle motions. An orbital rate can be applied for stabilizing the line-of-sight to a point on the surface of the earth. The hand controller can be used for target acquisition and trim commands based on the display from a table mounted TV or an experiment. When switch A is in its alternate position, the table can be positioned directly by an experiment error signal with damping provided by the gimbal rate loop. When switch B is also in its alternate position, the table will be driven to reposition its gimbals to zero, or slaved to any other instrument or pointing direction specified by a set of two Euler angles.

The pointing capability of the experiment table has been discussed with the assumption that an ideal error signal or pointing reference is available. In other words, the sensor or reference error is neglected and the pointing error results from the inability of the torquer control loop to null the error signal. This is a reasonable assumption when a good error signal is available directly from the experiment. However, when an external sensor is necessary, the pointing accuracy is degraded by any misalignment between the experiment and sensor.

Table 3 gives the estimated pointing errors for experiments which are controlled by the table. The table with nominal preparation refers to the fact that no special attempt was made to balance the load other than a reasonably symmetrical mounting of experiments on the inner gimbal ring (C.G. error of ±2 in.). This primarily affects jitter rate. The case for which the gimbal error signal is obtained from a sensor mounted on the inner gimbal (as in Skylab) results in a large reference error of about 1 arc min. A better estimate of this value should be available after the Skylab mission. The table which has precision balanced loads (C.G. error of ±0.4 in.) and a good error

TABLE 3. ESTIMATED POINTING ERRORS FOR SORTIE EXPERIMENTS

CONTROL TECHNIQUE	SENSOR LOCATION	ERROR TYPES			
		A REFERENCE	B STABILITY	POINTING A + B	JITTER RATE
● SHUTTLE ACPS:					
● LARGE THRUSTERS	SHUTTLE GN & C	$\pm 0.5^{\circ}$	$\pm 0.5^{\circ}$	$\pm 1.0^{\circ}$	$\pm 0.1^{\circ}/s$
● SMALL THRUSTERS	SHUTTLE GN & C	$\pm 0.5^{\circ}$	$\pm 0.1^{\circ}$	$\pm 0.6^{\circ}$	$\pm 0.01^{\circ}/s$
	EXPERIMENT FIXED	$\pm 0.1^{\circ}$	$\pm 0.1^{\circ}$	$\pm 0.2^{\circ}$	$\pm 0.01^{\circ}/s$
● CMG'S:					
● SKYLAB APPLICATION	SKYLAB RACK	$+0.1^{\circ}$	$\pm 0.02^{\circ}$	$\pm 0.12^{\circ}$	$\pm 0.0167^{\circ}/s$
● SHUTTLE APPLICATION	INTERNAL TO EXP.	NEGLIGIBLE	$\pm 0.02^{\circ}$	$\pm 0.02^{\circ}$	$\pm 0.01^{\circ}/s$
			(± 72 $\widehat{sec}$)	(± 72 $\widehat{sec}$)	(± 36 $\widehat{sec}/s$)
● EXPERIMENT TABLE:					
● NOMINAL PREPARATION	INNER GIMBAL	± 60 $\widehat{sec}$	± 2.5 $\widehat{sec}$	± 62.5 $\widehat{sec}$	± 5 $\widehat{sec}/s$
● PRECISION BALANCING	INTERNAL TO EXP.	NEGLIGIBLE	± 0.5 $\widehat{sec}$	± 0.5 $\widehat{sec}$	± 1 $\widehat{sec}/s$

● ERRORS WHICH RESULT FROM ROLL ABOUT LINE OF SIGHT WILL BE A FUNCTION OF VEHICLE AIRFRAME STABILITY.

signal directly from the experiment can probably achieve a pointing accuracy below 1 arc sec and a jitter rate of about 1 arc sec/s. Any pointing requirement which exceeds these values must be supplied by internal control of experiment optics.

SIMULATION OF THE SORTIE MISSION POINTING PROBLEM

The problem of precision pointing from a thruster controlled Shuttle has been investigated by modeling the ACPS characteristics and the EPC System of Skylab on an analog computer. Figure 6 illustrates the problem and defines the symbols used in the study. The ACPS characteristics included deadband, minimum on time, and optimized control gains. The EPC model contained flex pivot spring torques, cable hystersis, motor deadband, first order lag and torque limiting. The simulation diagram is shown in Figure 7. This is a single degree of freedom simulation with sensor errors and noise considered to be negligible. A single axis representation is considered to be adequate for this study. However, the introduction of nonideal sensor characteristics into the EPC control loop would degrade these results. Therefore, this study should reflect the basic capability of the EPC servo loop when operating with an ideal sensor.

The Phase B orbiter mass characteristics and thruster configuration were used for this study. However, the results are just as applicable to the external tank orbiter since the study was made for a range of thrust levels which includes representative angular acceleration values for that configuration.

Figure 8 shows the effect of thrust level on EPC pointing and stability. Time intervals of 1 and 10 s are shown by the pulses at the top of the page. The thrust values are for the Phase B orbiter with two thrusters operating in a couple. Therefore, the angular acceleration is very high for the first case (2000 lb thrust). Angular acceleration ($\ddot{\phi}_s$), velocity ($\dot{\phi}_s$) and position (ϕ_s) of the Shuttle airframe are shown on the first three traces. Angular position (δ) and velocity ($\dot{\delta}$) of the EPC are shown in the final two traces. The Shuttle is given a small initial rate to induce typical thruster operation. This thruster operation occurs as ϕ_s reaches the 1 degree deadband. The thruster operation appears as spikes of $\ddot{\phi}_s$ with corresponding changes in level of ϕ_s. The complete explanation of the δ response will be given in Figure 9. However, note that the angle does not exceed 1 arc sec even for this large thrust level. The

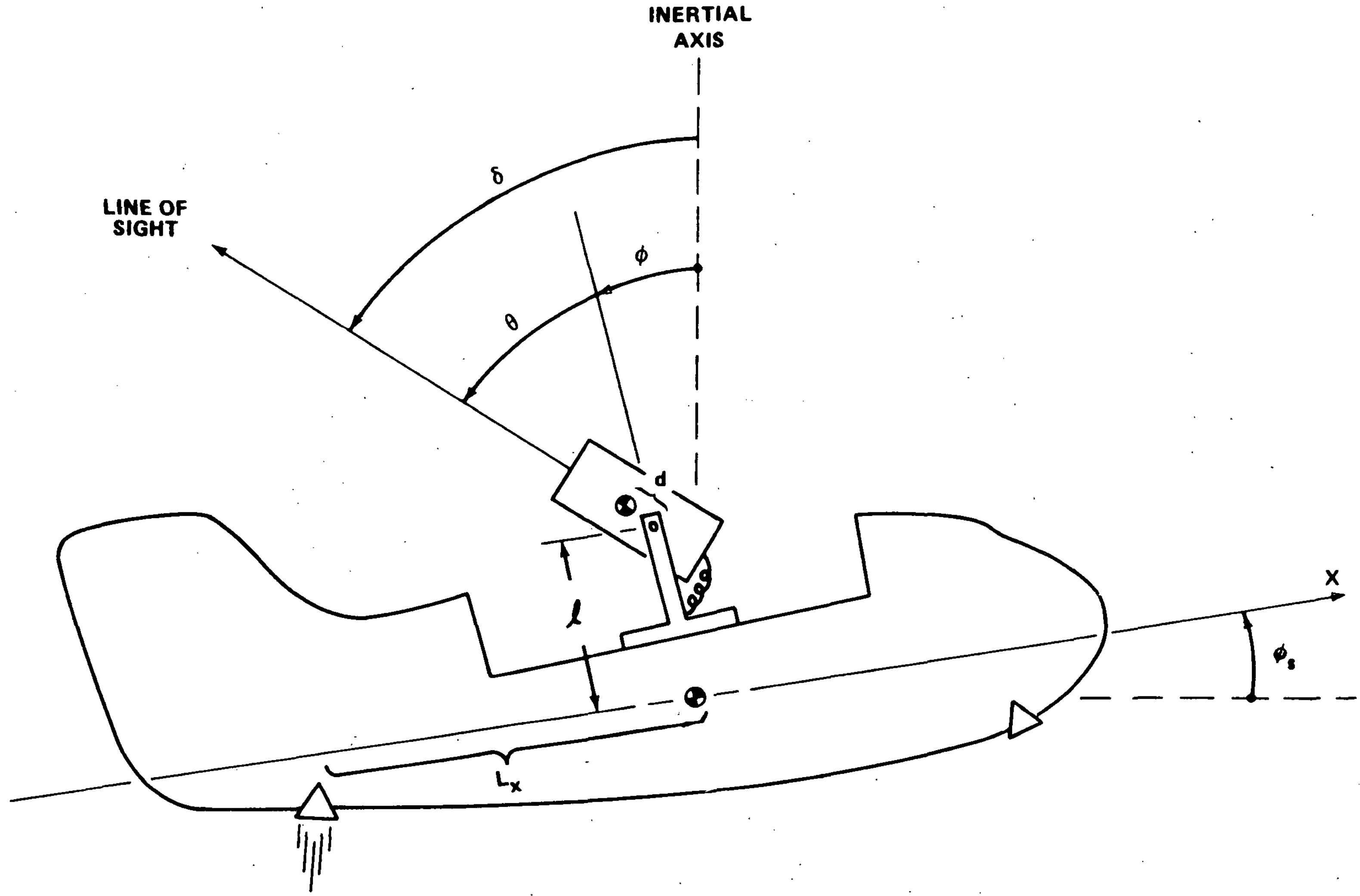

Figure 6. Definition of symbols.

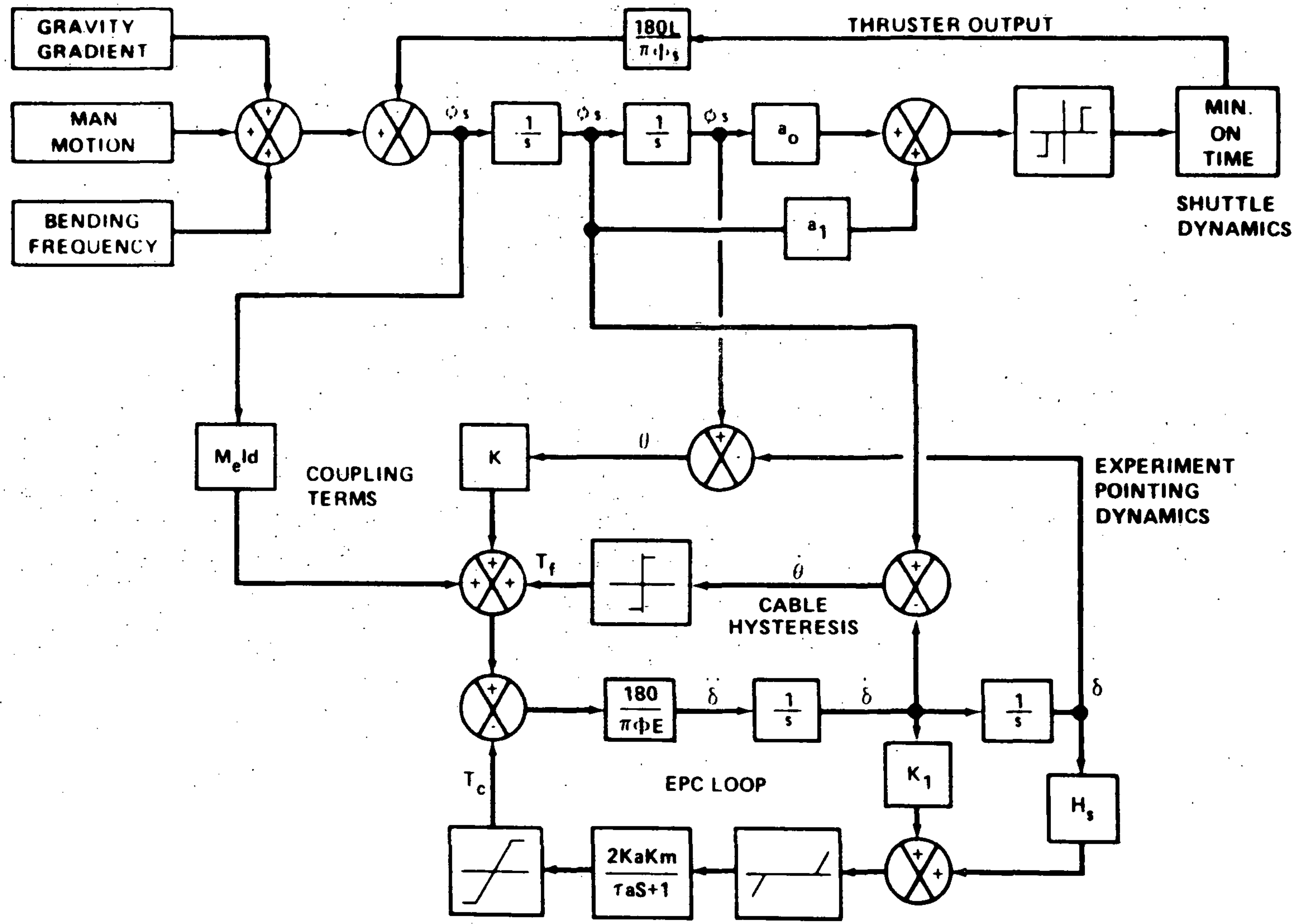

Figure 7. Simulation diagram: Shuttle with Skylab Experiment Pointing System.

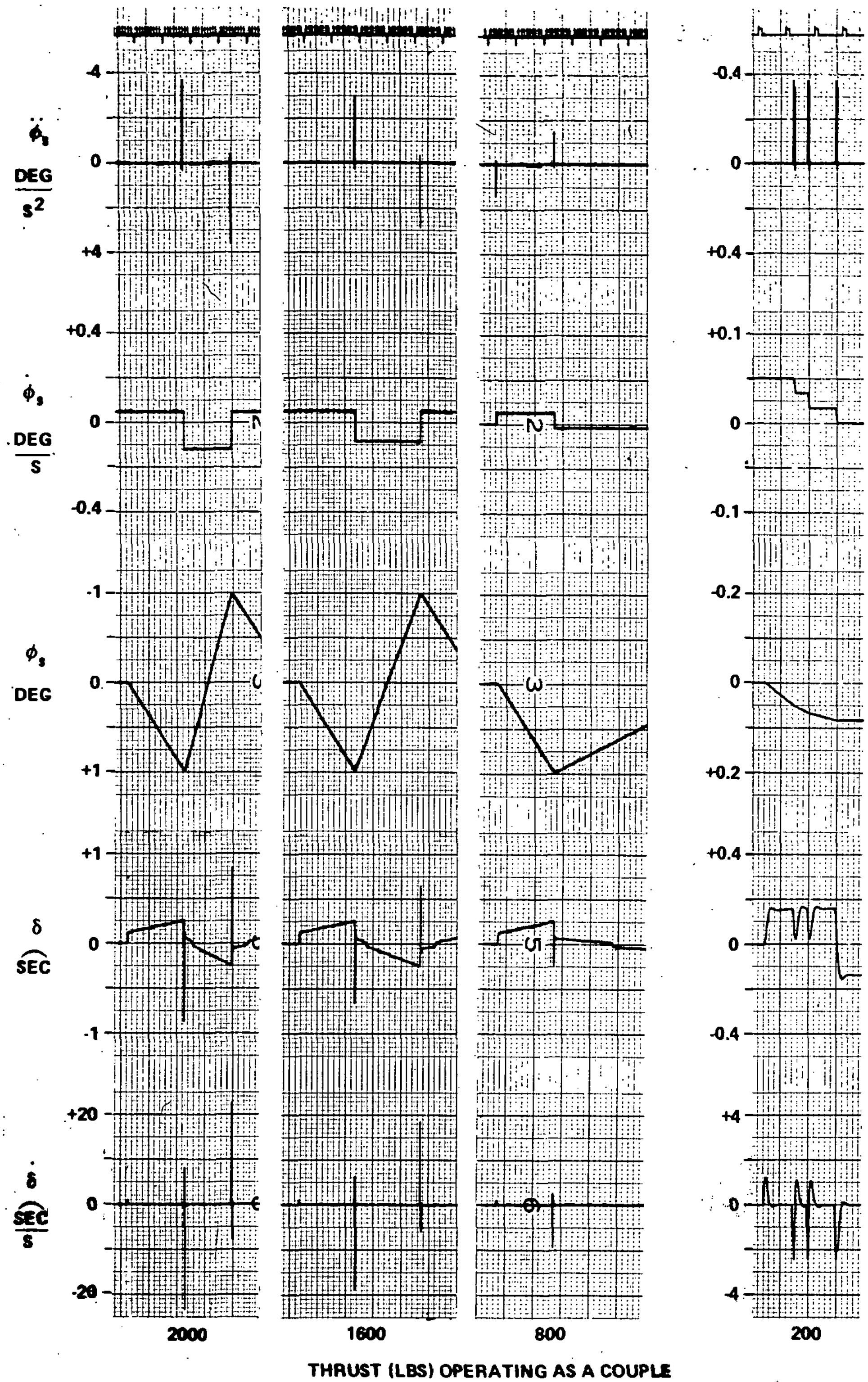

Figure 8. Effect of thrust level on experiment pointing and stability.

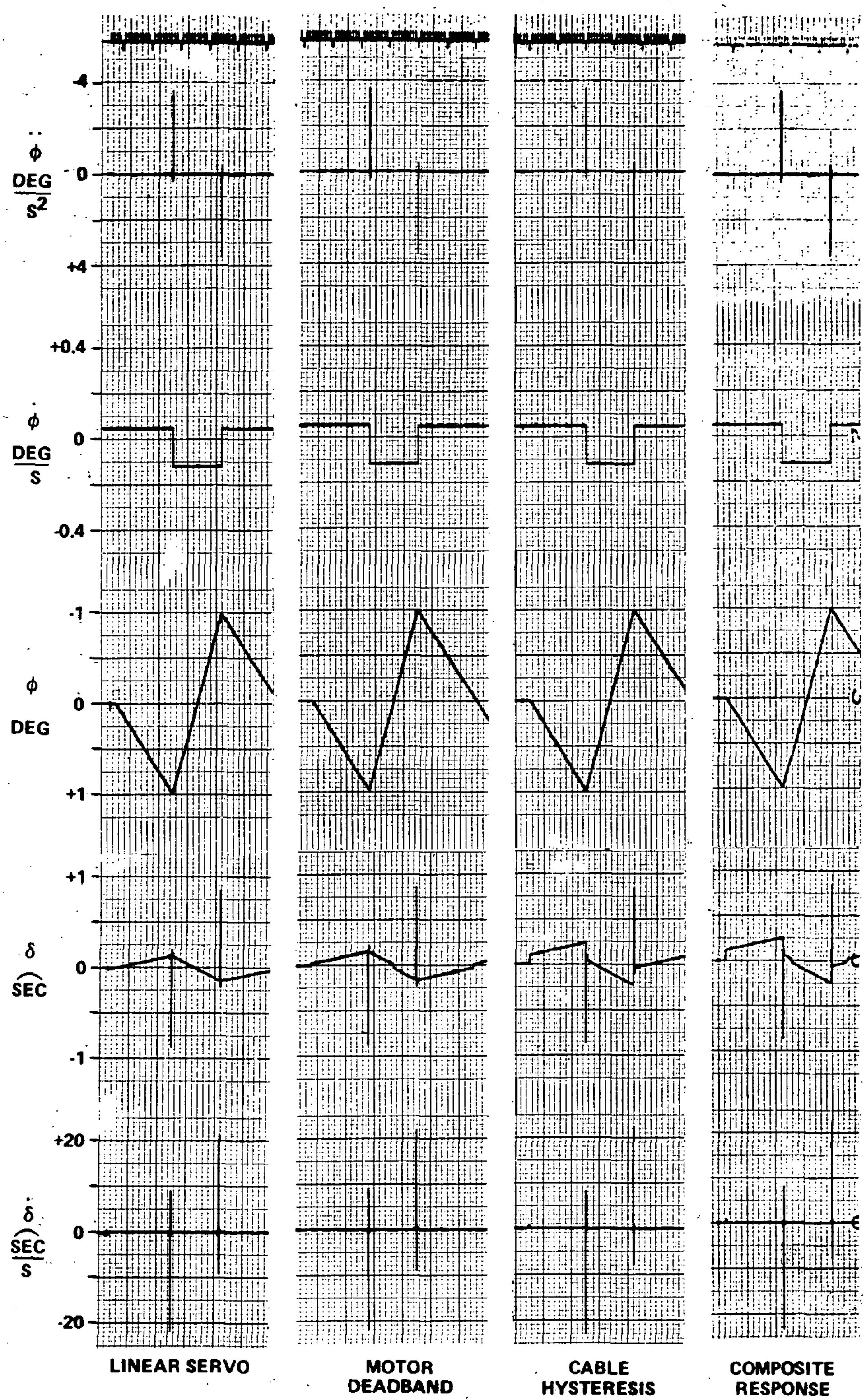

Figure 9. Effect of nonlinear characteristics on Experiment Pointing System.

rate ($\ddot{\delta}$), which is relatively high at about 21 arc sec/s would not meet the criteria for most precision pointing tasks. As thrust levels are decreased, the reduction in disturbance to the EPC is obvious. The final case (200 lb thrusters) shows that the effect of thruster firings is less of a contributor to δ error than the nonlinearities of the EPC servo loop. The $\dot{\delta}$ values are now down to 2.5 arc sec/s.

Figure 9 illustrates the effect of nonlinearities on the EPC response characteristics. The first case is for an ideal, linear servo. The ramp on δ is the result of the flex pivot spring constant and the angular deviation between the EPC and the Shuttle ($\sim \phi_S$). The spikes on δ and $\dot{\delta}$ result from the $M_E \ell d$ coupling term. In other words, the magnitude of Shuttle angular acceleration which couples over into the EPC is the product of EPC mass (M_E), length from Shuttle C.G. to EPC gimbal point (ℓ), and offset of EPC C.G. relative to its gimbal point (d). This is an important expression since a reduction in any of these parameters will proportionately reduce the disturbing influence of the Shuttle on the EPC. This simulation was performed with $\ell = 10$ ft and d = 1 in.

The second case in Figure 9 shows the effect of adding motor deadband to the linear servo. There is only a relatively minor change to the δ trace. However, cable hysteresis, which results from the flexing of cables between the Shuttle and EPC, makes a significant change to the $\dot{\delta}$ trace. The composite response case includes all the nonlinearities, first order lag and limiters.

Figure 10 is a plot of EPC position error (δ) and jitter rate ($\dot{\delta}$) as a function of Shuttle angular acceleration. The linear decrease of the curves represents the reduction in the spikes which couple into the EPC from thruster operation. However, when the angular acceleration gets below about 0.5 degree/s^2, the nonlinearities of the EPC predominate and system errors maintain a constant magnitude. This level represents the best stability and jitter rate that can be obtained from this particular system for an ideal sensor and minimal disturbances.

Figure 11 illustrates the transient response of the EPC system to a thruster firing. The torquer output (T) and EPC angular acceleration ($\ddot{\delta}$) are shown on the bottom two traces. The first run was made at 0.5 mm/s and was then increased to 50 mm/s for the second run to show the detailed response.

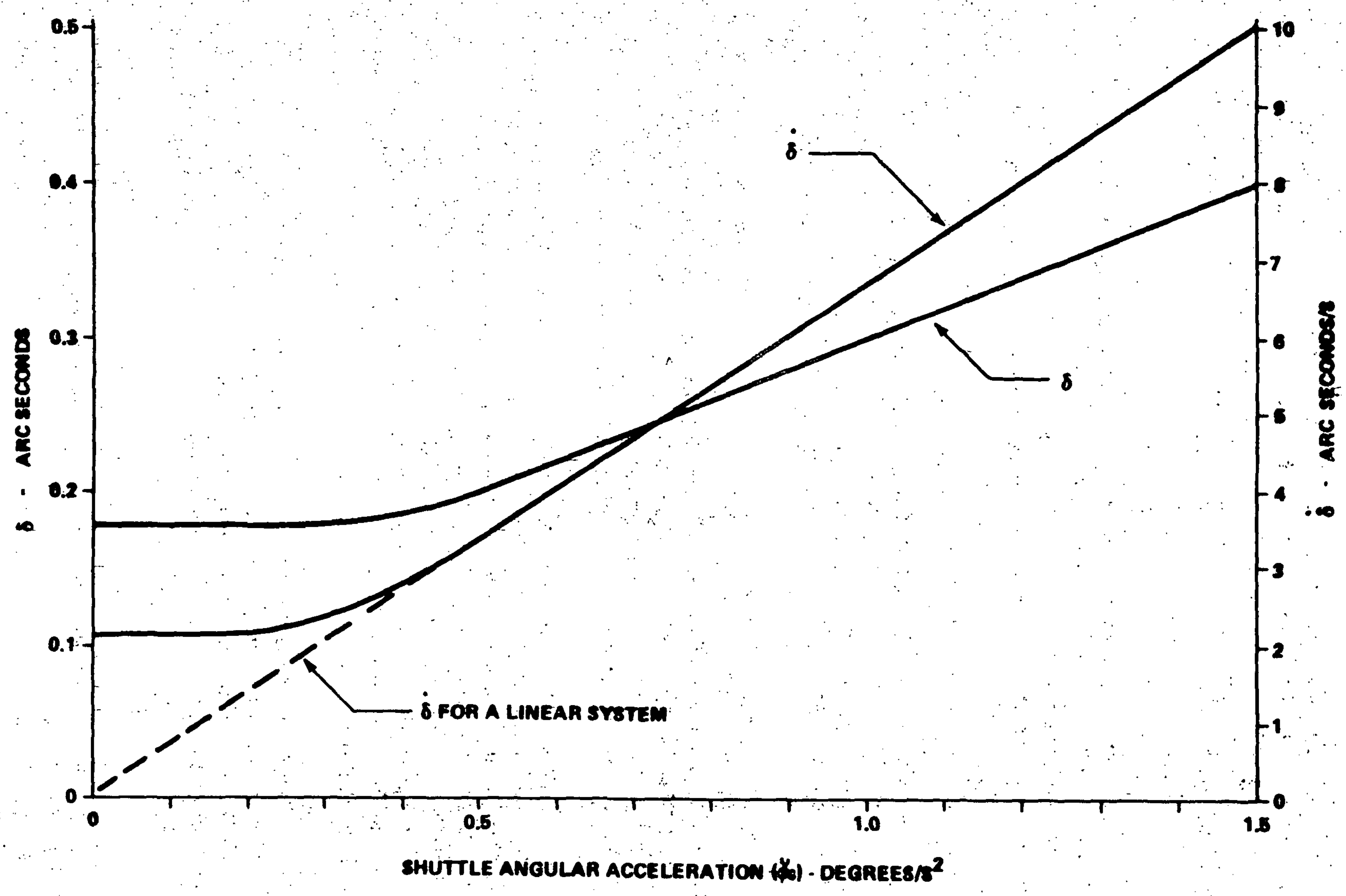

Figure 10. Variation of EPC system errors with Shuttle angular acceleration.

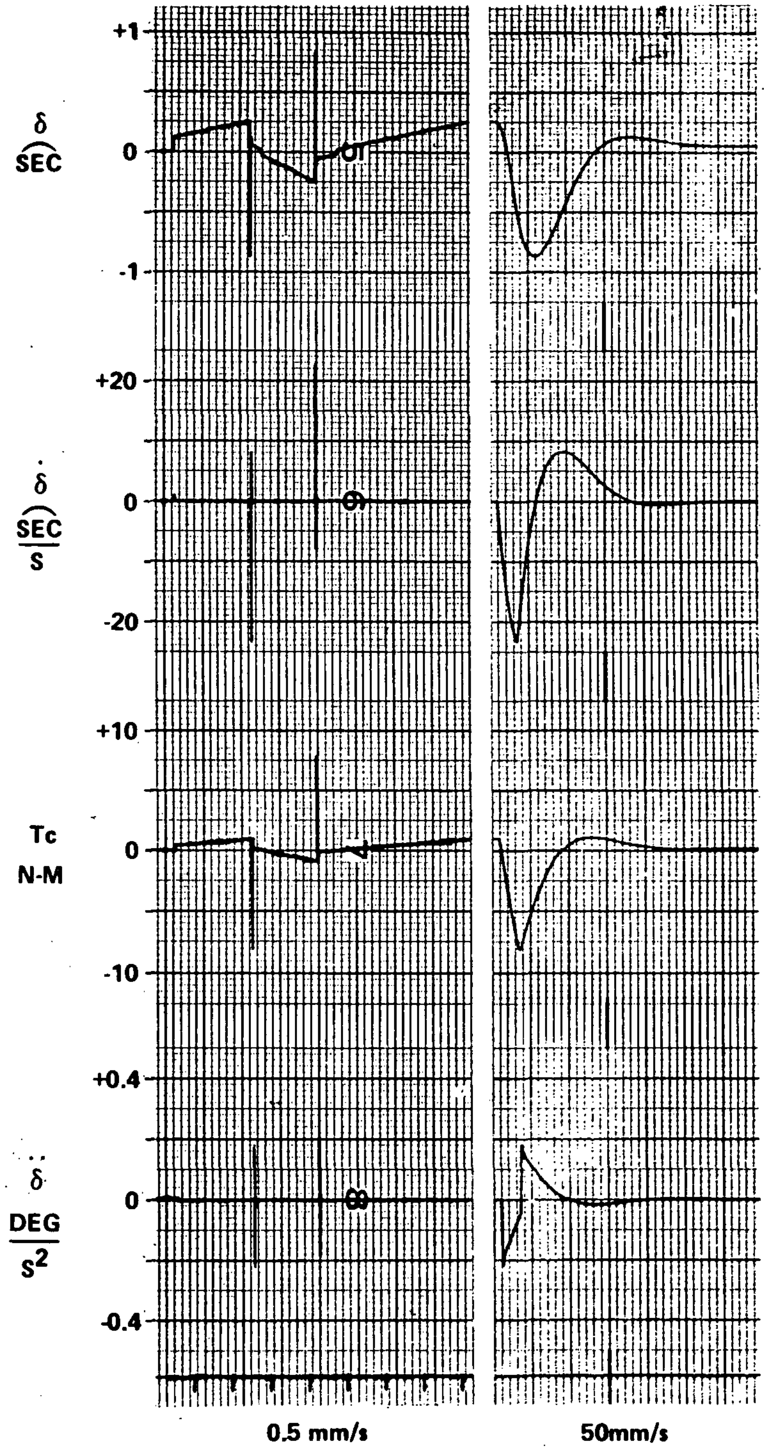

Figure 11. EPC transient response.

Figure 12 shows the EPC response to the firing of a 20 lb thruster. These are not minimum impulse firings (0.05 s). The on time is about 3 s as a result of nonoptimum control gains on the Shuttle. However, it does illustrate the point that EPC errors remain at the level established by the servo loop nonlinearities.

The body bending and man motion disturbances were introduced into this simulation as a disturbing torque simply to get some preliminary information on the nature of these disturbances. The modeling techniques and estimated input values make these results invalid for quantitative comparison. However, the results are shown in Figure 13 to illustrate the characteristic response. Body rates are attenuated by a factor of about twenty between the Shuttle and EPC. Man motion is apparently not as significant for the Sortie missions as for Skylab because of the larger moments of inertia.

CONCLUSIONS

The Sortie mode offers a convenient and economical means of performing many orbital experiments. It should be a reasonable follow-on for Skylab type experiments and an alternative to the Convair 990 airborne laboratory with greatly increased capability. The Sortie mode is uniquely qualified for many earth observation missions. Our studies show that the stability potential exists even for performing many celestial pointing missions with relatively minor modifications to the basic Shuttle control system. The flexibility and versatility of the proposed pointing control system should permit the Shuttle to operate as an orbital observatory with an unusually wide range of applications.

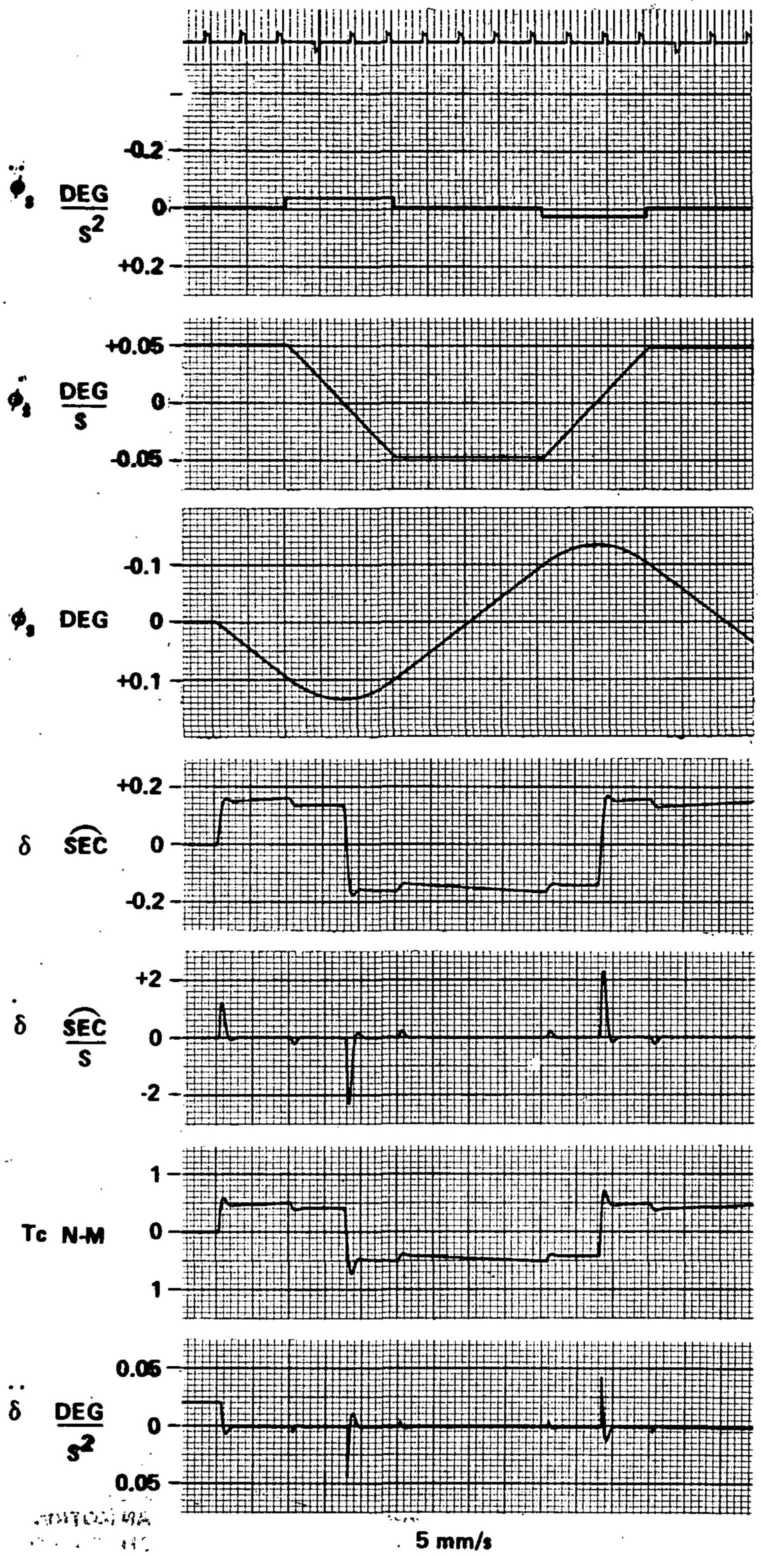

Figure 12. EPC response to a 20 lb thruster.

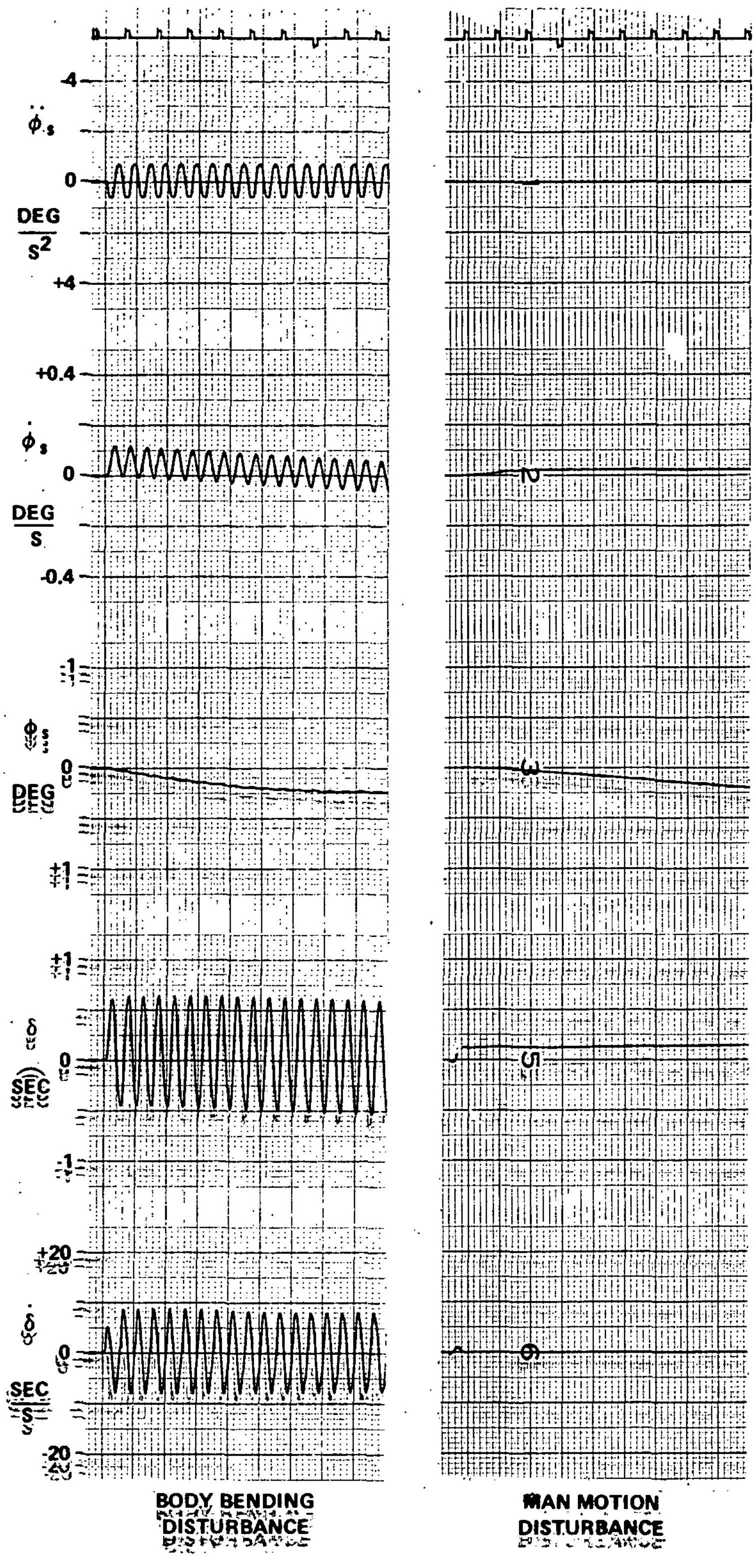

Figure 13. Effect of disturbances on Experiment Pointing System.

BIBLIOGRAPHY

Chubb, W. B. and Epstein, Michael: Application of Control Moment Gyros in the Attitude Control of the Apollo Telescope Mount., AIAA Paper No. 68-866, August 1968.

Chubb, W. B.; Schultz, D. N.; and Seltzer, S. M.: Attitude Control and Precision Pointing of the Apollo Telescope Mount., AIAA Paper, June 1967.

Nein, Max E. and Olivier, Jean R.: Techniques for Conducting Scientific Research and Application Studies from an Orbiting Space Shuttle. Paper presented at the XXII International Astronautical Congress in Brussels, Belgium, September 1971.

APPROVAL

EXPERIMENT POINTING CONTROL DURING SPACE SHUTTLE SORTIE MISSIONS

By P. D. Nicaise

The information in this report has been reviewed for security classification. Review of any information concerning Department of Defense or Atomic Energy Commission programs has been made by the MSFC Security Classification Officer. This report, in its entirety, has been determined to be unclassified.

This document has also been reviewed and approved for technical accuracy.

David N. Schultz

DAVID N. SCHULTZ
Chief, Navigation and Control Systems Branch

Fred E. Digesu

FRED E. DIGESU
Chief, Electronics and Control Division

Erich E. Goerner

ERICH E. GOERNER
Director, Preliminary Design Office

James T. Murphy

JAMES T. MURPHY
Acting Director, Program Development

DISTRIBUTION

INTERNAL

DIR
Dr. Rees

DEP-T
Dr. Lucas

AD S
Dr. Stuhlinger

S&E-DIR
Dr. Weidner
Dr. Haeussermann

S&E-EA-DIR
Dr. McDonough
Mr. Paludan
Mr. Derrington

S&E-S/P-A
Mr. Hammers
Mr. Blackstone
Mr. Wolf
Mr. Jenke

S&E-AERO-DIR
Dr. Geissler

S&E-AERO-M
Mr. Lindberg

S&E-AERO-D
Dr. Worley
Mr. Craighead

S&E-ASTN-DIR
Mr. Heimburg
Mr. Tessmann

S&E-ASTR-DIR
Mr. Moore

S&E-ASTR-X
Mr. Cagle

S&E-ASTR-A
Dr. Seltzer
Dr. Nurre
Dr. Jones
Mr. Kennel

S&E-ASTR-S
Mr. Wojtalik
Mr. Noel
Mr. Tanner
Mr. Mack

S&E-ASTR-C
Mr. Swearingen
Mr. White
Mr. Garrett

S&E-ASTR-SG
Mr. Brooks
Mr. Blanton
Mr. McMahen
Mr. Davis
Mr. Deaton
Mr. Fisher
Mr. Scott
Mr. Smith
Mr. McMillion
Mr. Chubb
Mr. Applegate
Mr. Smith
Mr. Thompson
Mr. Polites
Mr. Dawes

S&E-ASTR-SD
Mr. Scofield
Mr. Mink
Mr. Justice
Mr. Shelton

S&E-ASTR-G
Mr. Mandel
Dr. Doane
Mr. Jones

S&E-ASTR-GM
Mr. Kalange
Mr. Cornelius
Mr. Lominick
Mr. Golley
Mr. Krome

S&E-ASTR-GSF
Mr. Cook

SP-MGR
Mr. Godfrey

SP-EM
Mr. Hight

SS-MGR
Dr. Speer

SS-H-X
Mr. Perkins

MO-MGR
Mr. Kurtz

PD-DIR
Mr. Murphy
Mr. Jean
Mr. Downey
Dr. Mrazek

PD-SL
Mr. Trott
Mr. Palaora

PD-TR
Mr. Goodrum
Mr. Allen
Mr. Elms

PD-SA-DIR
Mr. Huber

PD-MP-DIR
Mr. Gierow

PD-CVT
Mr. Brooksbank
Mr. Hall

PD-MP-A
Mr. Olivier
Mr. Nein
Mr. Roberts

PD-DO-DIR
Mr. Goerner
Mr. Marshall
Mr. Heyer
Mrs. Kozub

PD-DO-M
Mr. Lane
Mr. Sanders
Mr. Schwartz

PD-DO-P
Mr. Goldsby
Mr. Sumrall
Mr. Bradford

PD-DO-S
Mr. Darwin
Mr. Blumrich
Mr. Wicks

PD-DO-E
Mr. Digesu
Mr. Harden
Mr. Boehme
Mr. Guidici
Mr. Arsement
Mr. Schultz
Mr. Green
Dr. Steincamp
Mr. Davis
Mr. Brandon
Mr. Weiler
Mr. Cole
Mr. Nicaise (30)

A&PS-MS-I
Mr. Remer

A&PS-MS-IP
Mr. Ziak (2)

A&PS-MS-IL
Miss Robertson (8)

A&PS-RU-DIR
Mr. Wiggins (6)

A&PS-MS-D
Mr. Garrett

A&PS-MS-H

A&PS-PAT
Mr. Wofford

A&PS-CP-M
Mr. Stevens

EXTERNAL

Manned Spacecraft Center
Houston, Tezas, 77058
Attn: Mr. G.T. Rice, EG-4

Kennedy Space Center
Kennedy Space Center, Florida 32899
Attn: Mr. C.M. LaPorte, LV-GDC-11
Mr. C. Whiteside, LV-GDC-11

General Dynamics Corporation
Convair Division
P.O. Box 1128
San Diego, California 92112
Attn: Mr. Daniel Chairappa (3)

Sperry Rand Corporation
716 Arcadia Circle
Huntsville, Alabama
Attn: Mr. Robert Shelton
Mr. Rufus Passwater

Bendix Corporation
Navigation and Controls Division
Teterboro, New Jersey 07608
Attn: Mr. Michael Epstein

Mr. Manuel Key
1101 West Thach Avenue
Apt. 9
Auburn, Alabama 36830

Scientific and Technical Information Facility (25)
College Park, Maryland 20740
Attn: NASA Representative (S-AK/RKT)